Hydrol. Earth Syst. Sci. Discuss., https://doi.org/10.5194/hess-2019-119
Manuscript under review for journal Hydrol. Earth Syst. Sci.
Discussion started: 27 March 2019

Hydrology and Earth System Sciences
Discussions

Understanding the potential of climate teleconnections to project future groundwater drought

Rust, William.[a]; Holman, Ian.[a]; Bloomfield, John.[b]; Cuthbert, Mark.[c]; Corstanje, Ron.[d]

a Cranfield Water Science Institute (CWSI), Cranfield University, Bedford MK43 0AL
b British Geological Survey, Wallingford, OX10 8ED
c School of Earth and Ocean Sciences, Cardiff University, Park Place, Cardiff, CF10 3AT
d Centre for Environment and Agricultural Informatics, Cranfield University, Bedford MK43 0AL

Abstract

Predicting the next major drought is of paramount interest to water managers, globally. Estimating the onset of groundwater drought is of particular importance, as groundwater resources are often assumed to be more resilient when surface water resources begin to fail. A potential source of long-term forecasting is offered by possible periodic controls on groundwater level via teleconnections with oscillatory ocean-atmosphere systems. However, relationships between large-scale climate systems and regional to local-scale rainfall, ET and groundwater are often complex and non-linear so that the influence of long-term climate cycles on groundwater drought remains poorly understood. Furthermore it is currently unknown whether the absolute contribution of multi-annual climate variability to total groundwater storage is significant. This study assesses the extent to which inter-annual variability in groundwater can be used to indicate the timing of groundwater droughts in the UK. Continuous wavelet transforms show how repeating teleconnection-driven 7-year and 16-32 year cycles in the majority of groundwater sites from all the UK's major aquifers can systematically control the recurrence of groundwater drought; and we provide evidence that these periodic modes are driven by teleconnections. Wavelet reconstructions demonstrate that multi-annual periodicities of the North Atlantic Oscillation, known to drive North Atlantic meteorology, comprise up to 40% of the total groundwater storage variability. Furthermore, the majority of UK recorded droughts in recent history coincide with a minima phase in the 7-year NAO-driven cycles in groundwater level, allowing the estimation of future drought occurrences on a multi-annual timescale. Long-range groundwater drought forecasts via climate teleconnections

present transformational opportunities to drought prediction and its management across the North Atlantic region.

1. Introduction

Inter-annual variability detected in hydrometeorological datasets has long been associated with systems of atmospheric-oceanic (climatic) oscillation, such as El Niño Southern Oscillation (ENSO) and the North Atlantic Oscillation (NAO). Such periodic teleconnection signals have been detected in rainfall (Luković et al. 2014), evapotranspiration (Tabari et al. 2014), air temperature (Faust et al. 2016), and river flow (Su et al. 2018; Dixon, et al. 2011); however these periodicities are often weak when compared to the finer-scaled (daily to seasonal) variability that is typical of hydrometeorological processes (Meinke et al. 2005). By contrast, groundwater systems are expected to be particularly susceptible to inter-annual teleconnection influence, given their sensitivity to long-term changes in rainfall and evapotranspiration (Bloomfield & Marchant 2013; Forootan et al. 2018; Van Loon 2015; Folland et al. 2015), and their ability to filter fine-scale variability in recharge signals (Dickinson et al. 2014; Velasco et al. 2015; Townley 1995). Consequently, recent studies have focused on the detection of long-term periodic cycles in groundwater levels in Europe (e.g. Holman et al. 2009; Holman et al. (2011); Folland et al. (2015); and Neves et al. (2019)), North America (e.g. Tremblay et al. (2011); Kuss & Gurdak (2014)) and globally (e.g. Wang et al. (2015); Lee & Zhang (2011)), and their relationships with climatic oscillations. An understanding of inter-annual perioidicity strength in groundwater level may provide an improvement in long-lead forecasting of hydrogeological extremes (Rust et al. 2018; Meinke et al. 2005; Kingston et al. 2006), in part, by enabling such cyclical behaviour to be projected into the future. This is particularly apparent of groundwater drought, which is known to result from multi-annual moisture deficits (Van Loon 2015; Van Loon et al. 2014; Peters et al. 2006). Therefore, it is critical to quantify the absolute strength of all periodicities within groundwater levels so that

57 the strength of inter-annual cycles, the influence of teleconnections, and their contribution
58 towards groundwater droughts can be understood.

59 Existing studies into groundwater teleconnections use quantitative methods to detect periodic
60 behaviour in groundwater datasets and often their relationship with time series of climate
61 indices (used to measure the strength and state of climate oscillations). Common quantitative
62 methods range from temporal correlation analysis (Knippertz et al. 2003; Szolgayova et al.
63 2014) to more complex periodicity detection and comparison. These latter methods include
64 Fourier transform, (Nakken, 1999, Pasquini et al. 2006), singular spectrum analysis (SSA)
65 (Kuss & Gurdak 2014; Neves et al. 2019) and wavelet transformations (Fritier et al. 2012;
66 Holman et al. 2011; Tremblay et al. 2011). The wavelet transform (WT) has been shown to be
67 particularly skilful at detecting inter-annual periodic behaviour in noisy hydrogeological
68 datasets; detecting the influence of the NAO, ENSO and Atlantic Multidecadal Oscillation
69 (AMO) on North American groundwater levels (Kuss & Gurdak 2014; Velasco et al. 2015), and
70 the NAO, East Atlantic pattern (EA) and Scandinavian pattern on European groundwater level
71 variability (Holman et al. 2011; Neves et al. 2019). However, in order to enhance inter-annual
72 periodicity detection, many studies have used data processing methods that remove or
73 supress variability at the higher end of the frequency spectrum (e.g. winter or annual averaging
74 or conversion of time series to cumulative departures from mean (Weber & Stewart 2004)).
75 Due to this data modification, it is currently unknown whether the absolute contribution of multi-
76 annual climate variability to total groundwater storage is significant. This limitation makes
77 assessment of systematic linkages between climatic oscillations and groundwater level
78 response problematic (Rust et al. 2018). As a result, the fundamental question of whether
79 inter-annual teleconnection cycles in groundwater level are sufficiently strong to influence
80 hydrogeological drought remains largely unanswered. Given the potential for improved long-
81 lead forecasting, quantification of inter-annual variability in groundwater level represents an
82 opportunity to support efficient infrastructure investment, systems of water trading (Rey et al.
83 2018) and robust planning for groundwater drought.

84 The aim of this paper is to assess the extent to which periodic behaviour in groundwater level
85 produced by teleconnections, may be used as an indicator for the timing of groundwater
86 droughts. In doing so, this paper develops and applies an improved method to describe and
87 characterise the absolute strength of periodic behaviour in groundwater level and its drivers
88 (rainfall and evapotranspiration). This aim will be met by addressing the following research
89 objectives:

90 1. Characterise dominant intra- and inter-annual periodicities in groundwater level
91 records across a range of aquifer types
92 2. Quantify the absolute strength of these inter-annual periodic groundwater level
93 oscillations compared to the total variability in groundwater levels
94 3. Qualitatively assess evidence for the control of climate teleconnections on identified
95 inter-annual periods
96 4. Assess the extent to which the timing of the inter-annual periodic groundwater level
97 oscillations align with recorded groundwater droughts

98 These objectives will be implemented on UK hydrogeology records, given the considerable
99 coverage of recorded groundwater level data in time and across the country (Marsh &
100 Hannaford 2008) however the methodologies developed can be applied to any regions.

101

102 **5. Data and Methods**

103 2.1. Groundwater data

104 Groundwater level time series from 59 reference boreholes covering all of the major UK
105 aquifers, with record lengths of more than 20 years and data gaps no longer than 24 months,
106 have been assessed in the study. These recorded groundwater level hydrographs range from
107 21 to 181 years in length, with an average length of 53 years. The sites are part of the British
108 Geological Survey's Index Borehole network and, in addition to their data coverage, have been
109 chosen as they exhibit representative and naturalistic hydrographs with minimal impact from

Hydrol. Earth Syst. Sci. Discuss., https://doi.org/10.5194/hess-2019-119
Manuscript under review for journal Hydrol. Earth Syst. Sci.
Discussion started: 27 March 2019

Hydrology and Earth System Sciences
Discussions
Open Access
EGU

110 abstractions. They cover a range of unconfined and confined consolidated aquifer types and
111 have been categorised into 5 main aquifer groups; Chalk, a limestone aquifer comprising of a
112 dual porosity system with localized areas where it exhibits confined characteristics; Limestone,
113 characterised by fast-responding fracture porosity; Oolite characterised by highly fractured
114 lithography with low intergranular permeability; Sandstone, comprised of sands silts and muds
115 with principle inter-granular flow but fracture flow where fractures persist; and Greensands,
116 characterised by intergranular flow with lateral fracture flow depending on depth and formation
117 (Marsh & Hannaford 2008).

118

Hydrol. Earth Syst. Sci. Discuss., https://doi.org/10.5194/hess-2019-119
Manuscript under review for journal Hydrol. Earth Syst. Sci.
Discussion started: 27 March 2019

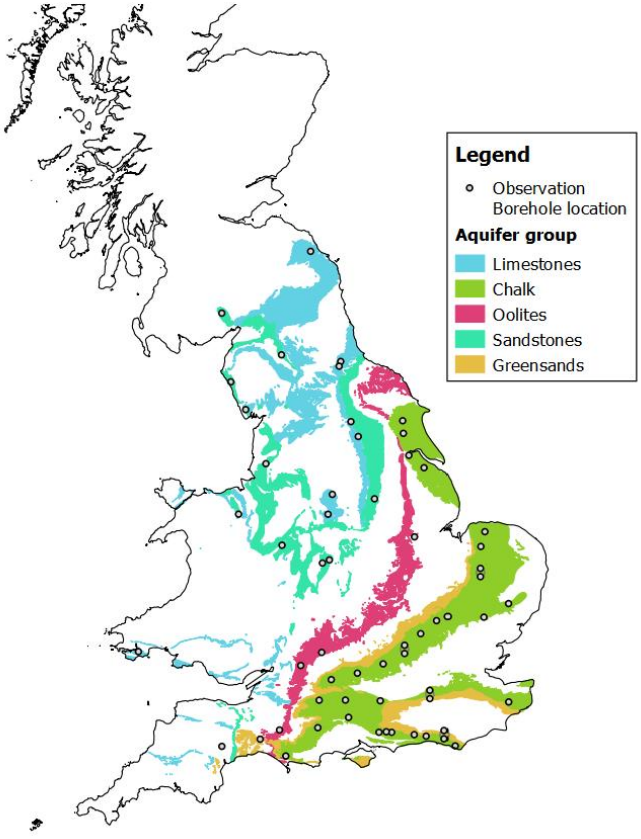

119

120 *Figure 1 - Location of the observation borehole locations used in this study. Boreholes within 0.5 km of another*
121 *have been displaced and denoted on a grey circle for visibility.*

122

123 2.2. Rainfall

124 Rainfall time series from the Centre of Ecology and Hydrology's CEH-GEAR 1km gridded
125 rainfall dataset (Tanguy et al. 2016), which is based on spatio-temporal interpolation of daily
126 rain gauge totals between 1890 and 2017, was used. However, relatively few rainfall stations
127 exist prior to 1950 that were used for this interpolation; as such data prior to 1950 was not
128 used in this analysis. Monthly rainfall series have been calculated for each borehole from the
129 1km grid cell in which they are located, as geospatial data on areas of groundwater recharge
130 connected to specific observation boreholes does not exist. This dataset may contain artefacts
131 as a result of the spatio-temporal interpolation, in comparison to station data. However the

use of rainfall data in this study is to provide a broad understanding of rainfall periodicities to supplement those from groundwater level data. As such, this interpolated dataset is deemed appropriate.

2.3. Potential Evapotranspiration (PET)

Monthly PET series for each borehole have been derived from the Centre of Ecology and Hydrology's CHESS-PE 1km gridded dataset of calculated daily PET values. The PET values, between 1960 and 2015, were calculated using the Penman-Monteith equation, with meteorological data taken from the CHESS gridded meteorological dataset. Details on the underlying observation datasets and interpolation methods can be found in Robinson et al. (2016). This data has been used previously to study long-term trends in hydrological variability (Robinson et al. 2017).

2.4. Methods

2.4.1. Data pre-processing

In this study we use the continuous wavelet transform (CWT) to produce a time-averaged frequency spectrum for each borehole hydrograph and co-located rainfall and PET time series.

For all datasets, gaps less than two years were infilled using a cubic spline to produce a complete time series for the CWT. This interpolated information was later removed from the time-frequency transformation (prior to time-averaging) to ensure that the data infilling had minimal effect on the final spectrum. For time series with gaps greater than two years, the shortest time period before or after the data gap was removed to produce one complete record. Individual rainfall and PET time series were trimmed to match the length of the corresponding borehole level time series. All time series were centred on the long-term mean and normalized to the standard deviation to produce a time series of anomalies. Unlike most

157 previous studies, no high- or low-band filtering was undertaken on the datasets, ensuring all
158 information on periodic variability was preserved. This approach ensures that the Proportion
159 of a periodicity to the variance (standard deviation) of the original dataset is not modified.

160 2.4.2. Continuous Wavelet Transform.

161 Following the data pre-processing steps, a CWT was applied to quantify the time-averaged
162 frequency spectra of the rainfall, PET and groundwater datasets. The CWT has been used
163 to assess long term trends and periodicities in many hydrological datasets including rainfall
164 (Rashid et al. 2015), river flow (Su et al. 2017), and groundwater (Holman et al. 2011; Kuss
165 & Gurdak 2014). We use the package "WaveletComp" produced by Rosch & Schmidbauer
166 (2018) for all transformations in this paper.

167 The continuous wavelet transform, W, consists of the convolution of the data sequence (x_t)
168 with scaled and shifted versions of a mother wavelet (daughter wavelets):

$$W(\tau, s) = \sum_t x_t \frac{1}{\sqrt{s}} \psi * \left(\frac{t - \tau}{s}\right) \quad \text{(Eq. 1)}$$

169 where the asterisk represents the complex conjugate, τ is the localized time index, s is the
170 daughter wavelet scale and dt is increment of time shifting of the daughter wavelet. The
171 choice of the set of scales s determines the wavelet coverage of the series in its frequency
172 domain. The Morlet wavelet was favoured over other candidates due to its good definition in
173 the frequency domain and its similarity with the signal pattern of the environmental time
174 series used (Tremblay et al. 2011; Holman et al. 2011).

175 The CWT produces a time-frequency wavelet power spectrum for each time series. Within
176 the time-frequency spectra, a cone of influence (COI) is used to denote those parts that are
177 affected by edge-effects, where estimations of spectral power are less accurate. Therefore
178 only data from within COI were averaged over time to produce a time-average wavelet power
179 spectrum for frequency bands from 6 months up to 64 years. Wavelet power spectra were
180 then normalised to the maximum average wavelet value so that the frequency distribution of

each site can be directly compared. The normalized average wavelet power spectra (herein referred to as the wavelet power spectra) provide a comparative measure of the strength of the range of periodicities within frequency space.

2.4.3. Significance testing

As Allen and Smith (1996) demonstrate, geophysical datasets can exhibit pseudo-periodic behaviour as a result of their lag-1 autocorrelation (AR1) properties. Datasets with greater AR1 tend to have spectra biased towards low frequencies, thus they are described as containing red noise (Allen et al. 1996; Meinke et al. 2005; Velasco et al. 2015). In order to assess the likelihood that a periodic signal is the result of internal (red) noise within the data, significance of the red noise null hypothesis was tested. For this, 1000 randomly constructed synthetic series with the same AR1 as the original time series were created using Monte Carlo methods. Wavelet spectra maxima from these represent periodicity strength that can arise from a purely red noise process. Wavelet powers from the original dataset that are greater than these “red” periodicities are therefore considered to be driven by a process other than red noise, thus rejecting the null hypothesis. Here, while a 95% Confidence Interval (CI) (<= 0.05 alpha values) is identified, we report on the full range of alpha results to provide a detailed assessment of the likelihood of external forcing on periodic behaviour.

2.4.4. Time reconstruction

In order to assess the characteristics of periodicities over time, we employ a reversal of the wavelet transform (wavelet reconstruction) to convert selected periodic domains back into a time series of normalised anomalies. Period bands were selected where the frequency spectra identified shared wavelet power (and significance) between groundwater, rainfall and PET, indicating a wide-spread signal presence at these bands.

The reverse wavelet transform is given by:

Hydrol. Earth Syst. Sci. Discuss., https://doi.org/10.5194/hess-2019-119
Manuscript under review for journal Hydrol. Earth Syst. Sci.
Discussion started: 27 March 2019

$$(x_t) = \frac{dj \cdot dt^{1/2}}{0.776 \cdot \psi(0)} \sum_s \frac{Re(W(.,s))}{s^{1/2}} \quad \text{(Eq. 2)}$$

Where *dj* is the frequency step and *dt* is the time step.

Negative phases of these time-reconstruction anomaly time series were compared to episodes of recorded wide-scale hydrogeological drought (provided by Marsh et al. (2007) and Todd et al. 2013)), to assess the relationships between inter-annual variability in groundwater and groundwater droughts.

2.3.5 Periodicity strength quantification

While the wavelet power spectra from the CWT provide an estimate of the relative strength of periodicities compared to the total frequency spectra, they do not provide an absolute measure of a periodicities contribution to total groundwater variability (which includes noise and non-periodic information). As such the percentage contributions of each time-reconstruction have been calculated. Since the datasets were normalised to the standard deviation of the raw data prior to the CWT, the standard deviations of the reconstructed anomaly time series represent the proportion of the original standard deviation as a decimal percentage.

Hydrol. Earth Syst. Sci. Discuss., https://doi.org/10.5194/hess-2019-119
Manuscript under review for journal Hydrol. Earth Syst. Sci.
Discussion started: 27 March 2019

Hydrology and Earth System Sciences
Discussions
Open Access
EGU

Figure 2 - Normalised average wavelet power spectra (left) and wavelet power significance alphas (right) for monthly groundwater levels in the 59 index boreholes (grouped by aquifer type). In the right-hand figure, boxes outlined in white are those powers that are significant over red noise to a 95% confidence interval (a <= 0.05).

Hydrol. Earth Syst. Sci. Discuss., https://doi.org/10.5194/hess-2019-119
Manuscript under review for journal Hydrol. Earth Syst. Sci.
Discussion started: 27 March 2019

Hydrology and Earth System Sciences
Discussions
Open Access
EGU

Figure 3 - Normalised average wavelet power spectra (left) and wavelet power significance alphas (right) for monthly rainfall time series for co-locations of the 59 index boreholes. In the right-hand figure, boxes outlined in white are those powers that are significant over red noise to a 95% confidence interval (a <= 0.05).

Hydrol. Earth Syst. Sci. Discuss., https://doi.org/10.5194/hess-2019-119
Manuscript under review for journal Hydrol. Earth Syst. Sci.
Discussion started: 27 March 2019

Figure 4 – Overlaid reconstructions of the three key periodic domains found across the 59 groundwater wavelet spectra are shown. All periods (both significant and non-significant) within these bands have been displayed to allow for comparison of period strength and phase over time. Areas shaded blue represent periods of significant droughts in the UK. Only reconstructions between 1955 and 2017 are shown to allow clearer comparison.

Hydrol. Earth Syst. Sci. Discuss., https://doi.org/10.5194/hess-2019-119
Manuscript under review for journal Hydrol. Earth Syst. Sci.
Discussion started: 27 March 2019

Hydrology and Earth System Sciences
Discussions
Open Access
EGU

Figure 5 – Overlaid rainfall (left) and PET (right) reconstructions of the three key periodic domains are shown. All periods (both significant and non-significant) within these bands have been displayed to allow for comparison of period strength and phase over time. Areas shaded blue represent periods of significant droughts in the UK. Only reconstructions between 1955 and 2017 are shown to allow clearer comparison.

Hydrol. Earth Syst. Sci. Discuss., https://doi.org/10.5194/hess-2019-119
Manuscript under review for journal Hydrol. Earth Syst. Sci.
Discussion started: 27 March 2019

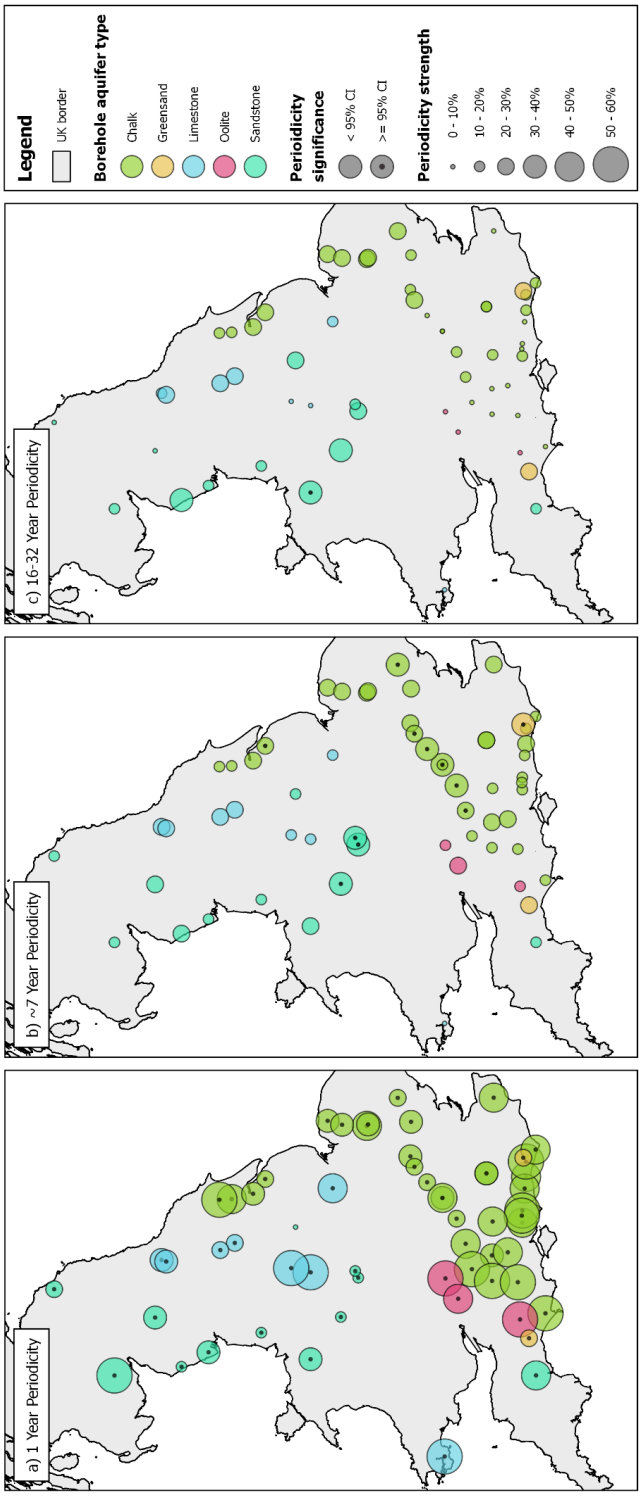

Figure 6 – Maps showing strength (percentage of the original time series standard deviation) and significance of the a) 1 year, b) ~7 year and c) 16-32 year periodicity bands. No periodicity strength was found to be above 60% of the original signal.

Hydrol. Earth Syst. Sci. Discuss., https://doi.org/10.5194/hess-2019-119
Manuscript under review for journal Hydrol. Earth Syst. Sci.
Discussion started: 27 March 2019

3. Results

3.1. Time-averaged wavelet power and significance over red noise

Wavelet power spectra (frequency strength) and alpha values (significance) for each of the 59 groundwater level and rainfall time series are displayed in figures 2 and 3 respectively. Wavelet power is analogous to the strength of the periodicity compared to other frequencies. Periodicities with alpha values less than or equal to 0.05 (95% CI) are highlighted. Bands of greater wavelet power and lower alpha values at periodicities of 1, ~7 and 16-32 year(s) can be seen across the majority of the groundwater and rainfall spectra for the 59 sites (herein referred to as P1, P7 and P16-32 respectively). PET wavelet spectra were found to have no notable or significant periodicity beyond seasonality (indicative of the UK's temperate climate), and are displayed in the supplementary material.

The annual cycle (P1) exhibited the greatest power across 43 of the 59 observation borehole spectra, with normalised wavelet powers ranging from 0.03 to 1 (mean of 0.84). Alpha values for P1 in the observation boreholes also showed the greatest likelihood of external forcing when compared to the other identified periodic domains (alpha values ranging from 0.00 to 0.94, mean of 0.017). All but one observation borehole (site 51 showed significant (95%) alpha values for P1 wavelet power. Lower than average P1 wavelet powers were most prevalent in the Sandstone lithology (6 out of 12 sandstone sites), Greensands (1 out of 2 sites) and to some extent, the Chalk (6 out of 35 sites). P1 wavelet power was generally lower across all the corresponding rainfall time series, which is expected given rainfall's established bias towards high-frequency variability (Meinke et al. 2005). Of those boreholes with lower P1 power in groundwater, most (e.g. 35, 59) show greater P1 powers in rainfall (and PET) indicating hydrogeological processes as the mechanism for weaker P1 periodicity. However, a small number (e.g. 38, 40 and 42) had similarly low P1 periodicity in the corresponding rainfall, indicating meteorological drivers for poor annual strength at these observation

boreholes (considering that PET showed little variance in P1 strength across the observation boreholes). PET spectra and alpha values showed a universally high P1 wavelet power.

The second greatest wavelet power across the groundwater boreholes was between 6 and 9 years, roughly centred on the 7 year periodicity (P7)). Maximum normalised groundwater wavelet powers ranging from 0.01 to 1 (average of 0.52) between boreholes were detected, and a corresponding band of lower than average alpha values (ranging from 0.01 to 0.99, mean of 0.34), indicating that this periodicity is likely to be driven by an external variance. Average P7 wavelet power values were greatest for Sandstone (0.68) and Greensands (1.00), and lower for Limestone (0.39) and Oolite (0.17). Chalk showed intermediate strength with the greatest range (0.01 to 1.00, mean of 0.50). Ten groundwater sites showed significant (95%) P7 wavelet powers (sites 1, 12, 14, 19, 26, 27, 49, 53, 55 and 59). While the P7 wavelet power in the corresponding rainfall data was considerably lower than those detected in groundwater level (ranging from 0.014 to 0.35, mean of 0.16), the alpha values are comparable with the P7 signal strength in groundwater. This indicates that P7 signals in rainfall are weak, but likely driven externally. Negligible wavelet powers and no significance was shown at the P7 band for corresponding PET data.

The final and second mode of common inter-annual wavelet power was the band between 16 years and 32 years (P16-32). P16-32 had an average wavelet power of 0.28 across all boreholes; ranging between 0.01 and 1. Similar to P7, the greatest wavelet power of P16-32 was found in the Sandstone (average of 0.58) and the Greensand (average of 0.64) aquifer types. Whereas Chalk, Limestone and Oolite showed relatively weaker signals (averages of 0.18, 0.32 and 0.03 respectively). Only one site in the groundwater (site 50) and five rainfall time series (sites 3, 11, 30, 34, 40) showed 95% significance over red noise in this periodicity band.

Hydrol. Earth Syst. Sci. Discuss., https://doi.org/10.5194/hess-2019-119
Manuscript under review for journal Hydrol. Earth Syst. Sci.
Discussion started: 27 March 2019

3.2. Reconstructed anomaly time series

The three main common period domains identified by the wavelet transform (P1, ~7 and 16-32 years) were reconstructed into anomaly time series using the reversed wavelet transform and are presented in figure 4 for groundwater levels and figure 5 for rainfall and PET. This was undertaken to allow investigation and comparison of periodic behaviour over time and to assess how these reconstructed periodic signals, within multiple sites across multiple aquifers, align with periods of historical groundwater drought. The behaviour of the multiple reconstructed groundwater level, precipitation and PET anomaly time series (in all three periodicity domains) were shown to be well-aligned in time, with positive (maxima) and negative (minima) phases occurring within comparable time. The only exception to this pattern was seen between 1970 and 1980 in the P7 reconstructions, where phases in the P7 reconstructions become misaligned. This was predominantly apparent in groundwater and to a lesser extent in rainfall. Positive and negative phases of the P7 reconstructions in PET were well-aligned for the entire time series.

Notable episodes of groundwater droughts in the UK were overlaid onto the reconstructed periods in figure 5 between 1955 and 2016. With the exception of the 1975-6 event, every episode of drought in this time period coincides with a negative phase of the reconstructed P7 groundwater anomalies. The 1975-6 drought (often used as a benchmark drought in the UK due to its wide-reaching impacts (Marsh et al. 2007)) occurred at a time of notable minima/maxima misalignment of the P7 period in groundwater, and a period of negative anomaly in the P16-32 reconstructions. Most recorded major droughts in the UK appeared to occur irrespective of the state of the P16-32 anomaly, with droughts occurring in minima and maxima of this reconstruction.

3.3. Percentage standard deviation

The percentage of the standard deviation in the original groundwater level signal represented by each reconstructed periodicity band is shown in figure 4 for all the observation boreholes.

322 The percentages are representative of the absolute strength of the periodicity compared to
323 the recorded data variance (standard deviation).

324 P1 represents the greatest average contribution to groundwater variability across all the
325 aquifer groups (Chalk: 41%, Limestone: 40%, Oolite: 52%, Sandstone: 26%, Greensand:
326 28%). While most sites show that P1 accounts for the greatest proportion of the standard
327 deviation, P7 is the dominant periodicity at 11 of the 59 sites (5 within Sandstone, 5 within
328 Chalk and 1 within Greensand), and P16-32 is the strongest cycle in 3 of the 59 sites (3 within
329 Sandstone and 1 within Limestone). P1 strength in the Chalk appears to be greatest in the
330 South of England, with weaker strengths in the South East and East. Aside from the Chalk,
331 there are no clear spatial patterns in P1 strength. P7 accounts for an average of 21.7% of
332 signal strength across all aquifer groups, ranging from 3.8% to 40% across the observation
333 boreholes. Spatial variance in P7 signal strength is less when compared to P1, although there
334 is a noted area of significance in Chalk of South East England (e.g. the Chiltern Hills and
335 Cambridgeshire), and a smaller cluster of P7 significance in the Sandstone of the central
336 England, where the greatest P7 strengths are found. P16-32 strengths are spatially focused
337 in Eastern England for the Chalk, and the central and north-western England for the
338 Sandstone. No clear patterns for the remaining aquifer groups is apparent for the 16-32 year
339 periodicity band.

340

Hydrol. Earth Syst. Sci. Discuss., https://doi.org/10.5194/hess-2019-119
Manuscript under review for journal Hydrol. Earth Syst. Sci.
Discussion started: 27 March 2019

4. Discussion

The aim of this study was to assess the extent to which inter-annual cycles in groundwater levels (produced by teleconnections with climate oscillations) may be used to indicate the timing of future groundwater extremes. To achieve this, the absolute strengths of groundwater periodicities have been quantified and compared to the timing of historical droughts in the UK. In this wide-scale study, our results show for the first time that long-term cycles in groundwater levels are a crucial contributor to overall groundwater level variability. Additionally we show that much of this periodic behaviour closely aligns with episodes of historical groundwater drought over the past 60 years. These findings move beyond previous groundwater teleconnection research in the UK (Holman et al. 2011) and internationally (Kuss & Gurdak 2014; Neves et al. 2019) to provide a robust measure of the absolute contribution of inter-annual periodicities to groundwater levels fluctuations. In the following, we discuss the findings presented in this paper within the context of the research objectives and the implications for improved water resource management.

4.1. Characterisation of signal presence and strength in groundwater level

Many studies have focused on the role of seasonality in defining groundwater variability, and the onset and severity of groundwater drought (Jasechko et al. 2014; Hund et al. 2018; Mackay et al. 2015; Ferguson & Maxwell 2010). While we show that the annual cycle is an important component of groundwater response, it is often not representative of overall behaviour, accounting for (on average) less than half of total groundwater level variability. Conversely, we show that inter-annual periodicities form an unprecedented proportion of total groundwater variability; with 41% of sites (24 out of 59) exhibiting inter-annual periodicity strength that is comparable to (within 10%), or greater than, seasonality. It is expected that the strength of inter-annual cycles in groundwater level will vary according to signal strength in recharge drivers (e.g. rainfall and evapotranspiration) and hydrogeological processes that lag or attenuate long-term changes in these recharge signals (Van Loon 2013; Van Loon 2015; Townley 1995; Dickinson et al. 2014). These two processes may explain the local differences

368 in signal strength between sites in aquifer types and geographically across the UK, as
369 displayed in our results. For instance, pronounced inter-annual variability (significant 7 year
370 cycles and stronger 16-32 year cycles) in the Chalk sites is generally associated with
371 catchments of thicker unsaturated zones, larger interfluves or areas of weaker corresponding
372 seasonality in rainfall (for example, the Chiltern Hills in South East England). These catchment
373 properties have been shown to dampen higher frequency variability between rainfall and
374 groundwater response due to storage buffers, thereby producing a sensitivity to inter-annual
375 variability (Peters et al. 2006; Van Loon 2013). Inter-annual cycles are also generally strong
376 for the granular porosity aquifers (Sandstone and Greensand); which is to be expected given
377 the influence of lower hydraulic diffusivity (typical of granular porosity flow) on the suppression
378 of high-frequency variability (Townley 1995). This also agrees with Bloomfield & Marchant
379 (2013) who document sensitivity to long-term accumulation in rainfall in UK Sandstone
380 aquifers. Conversely, the Limestone and Oolite aquifer types exhibit weaker inter-annual
381 periodicities in groundwater level, with strong seasonality. Townley (1995) and Price et al.
382 (2005) document that, due to their faster-responding fracture porosity with low storativity,
383 limestone lithographies have a lower damping capacity of finer-scale variability in recharge,
384 meaning they are able to respond in-time to the strong seasonality in PET and rainfall. We
385 demonstrate that inter-annual periodicity strength in groundwater level is the result of both
386 meteorological (principally rainfall) and hydrogeological processes. It might appear that our
387 results show lower percentage contributions of inter-annual periodicities to total groundwater
388 level variability than those presented in other studies (Kuss & Gurdak 2014; Neves et al. 2019;
389 Velasco et al. 2015). However as previous research has amplified lower frequencies in
390 groundwater level data spectra, the percentages reported in this study (which has not modified
391 the spectra of groundwater datasets prior to spectral decomposition (wavelet transform))
392 represent, for the first time, the absolute contribution of inter-annual variability to groundwater
393 level behaviour.

394

Hydrol. Earth Syst. Sci. Discuss., https://doi.org/10.5194/hess-2019-119
Manuscript under review for journal Hydrol. Earth Syst. Sci.
Discussion started: 27 March 2019

4.2. Evidence for teleconnection control on inter-annual groundwater variability

Here, we discuss the evidence that the inter-annual variability present in UK groundwater level records (as previously discussed) is the result of teleconnection influences with climatic oscillations. The conceptualisation of groundwater teleconnections of Rust et al (2018) suggests that a teleconnection between the oscillatory climate systems and groundwater level would be associated with;

a) an apparent and coherent inter-annual periodicity band within groundwater sites across a wide geographical area, that aligns with known inter-annual variability in indices of climatic oscillations (for instance, the 7-year periodicity of the NAO (Hurrell et al. 2003),
b) increased likelihood that this periodicity band is the result of an external influence, and not the result of internal red-noise variability of the groundwater level time series (as indicated by Allen et al. (1996) and Meinke et al. (2005))
c) comparable signals in rainfall as established drivers for inter-annual groundwater variability, and
d) broad alignment of minima and maxima of time-reconstructed inter-annual periodicities. Some fine-scale misalignment in groundwater periodicities is expected as a result of unsaturated and saturated zone lags between rainfall and groundwater response (Van Loon 2013; Peters et al. 2006; Dickinson et al. 2014; Cuthbert et al. 2019).

The majority of groundwater level hydrographs and corresponding rainfall profiles showed a coherent band of increased periodicity strength and periodicity significance principally around the 7-year frequency range and, to a lesser extent, the 16-32 year range. The 7 year periodicity closely compares to the principle 7-year periodicity documented in the strength of the NAO's atmospheric dipole, which has been associated with inter-annual periodicities in rainfall (Meinke et al. 2005) and groundwater globally (Tremblay et al. 2011; Kuss & Gurdak 2014; Holman et al. 2011; Neves et al. 2019). Additionally, the time-reconstructions show clear

422 temporal alignment of minima (with the exception of the 1975-6 period, which will be discussed
423 later), indicating the wide-spread coherent influence of a climatic teleconnection. As such, we
424 corroborate with existing research that documents the control of the NAO on UK rainfall
425 (Alexander et al. 2005; Trigo et al. 2004), and show new evidence of the wide-spread
426 propagation of inter-annual variability in rainfall through to spatio-temporal inter-annual
427 groundwater variability, conceptualised by Rust et al (2018).

428 While the NAO is known to be the dominant mode of winter climate variability in Europe
429 (López-Moreno et al. 2011; Alexander et al. 2005; Hurrell & Deser 2010), the second strongest
430 is provided by the East Atlantic (EA) pattern (Wallace & Gutzler 1981). The EA is similar in
431 frequency structure to the NAO but shifted southward, however it has been shown to exhibit
432 its own internal variability (Hauser et al. 2015; Tošić et al. 2016; (Moore et al., 2013).
433 Importantly, the EA has been shown to exhibit a 16-32 year periodicity (Holman et al, 2011),
434 and therefore aligns with the second strongest mode of inter-annual variability in groundwater
435 and rainfall documented in this study. Similar to the 7-year periodicity, the 16-32 year cycle
436 detected in groundwater levels shows an increased likelihood of external variance, and
437 temporal alignment of minima and maxima when reconstructed back into the time domain. As
438 such, we consider the EA to be the ultimate driver of the 16-32 year periodicity detected in UK
439 groundwater level. While the EA has received little focus in climate variability research
440 compared to the NAO, our findings here align with Krichak & Alpert (2005) who document a
441 multi-decadal control on UK and European precipitation through shifting phases of the EA,
442 and Holman et al (2011) who detected weak relationships between the EA and groundwater
443 levels in the UK. Comas-Brua and McDermotta (2014) suggest that much of the multi-decadal
444 climate variability (temperature and precipitation) in the North Atlantic region can be explained
445 by a modulation of the NAO by the EA, which may contribute to the spatial and temporal
446 variability seen in both the ~7 year and 16-32 year reconstructions across the borehole sites.
447 In summary, we assert that the inter-annual variability detected in UK groundwater and rainfall
448 data is likely the result of a climatic teleconnection with both the NAO and the EA. As such,

449 we document the first evidence of the absolute strength of both the NAO and the EA's control
450 on 7-year and 16-32 year varaibility in groundwater systems respecitvely.

451 **4.3. Teleconnections as indicators for groundwater extremes**

452 The final objective of this paper was to assess the extent to which the timing of inter-annual
453 periodic groundwater level oscillations align with the timing of recorded groundwater droughts.
454 To achieve this, documented periods of groundwater drought have been compared to
455 reconstructed periodicities within groundwater level. We show that every documented
456 groundwater drought between 1955 and 2014 aligns with a negative phase of the ~7 year
457 cycle detected in the majority of UK groundwater boreholes, with the exception of the 1975-6
458 drought. In addition to the strength of a ~7 year cycle in UK groundwater level previously
459 discussed, this alignment provides strong evidence that the NAO influences inter-annual
460 groundwater variability, resulting in groundwater drought on an approximate 7-year
461 recurrence. As mentioned, the only drought that does not fit this pattern is the 1975-6 drought,
462 which occurred during the only episode of temporal misalignment in the reconstructed 7-year
463 groundwater level periodicities. The 1975-6 drought is of particular interest for the UK as it is
464 often used as a benchmark drought, being one of the most severe droughts in recent history
465 (Marsh et al. 2007). (Rodda & Marsh 2011) attributed the severity of this drought to several
466 short-term influences (such as positive pressure anomalies driving dryer conditions), in
467 contrast to the multi-year accumulation of moisture deficits that typically result in
468 hydrogeological drought, particularly in the UK (Van Loon 2015; Bloomfield & Marchant 2013).
469 These assertions are apparent in our results, as the time reconstructions show negligible multi-
470 annual groundwater response occurring during this period, and an intense short-term
471 suppression of seasonality. As such, these results infer that the NAO did not directly modulate
472 the 1975-6 drought, agreeing with Parry et al (2011) who found no relationship with this
473 drought and the NAO. This potentially points to both the 1975-6 drought and the disrupted
474 NAO being modulated in parallel by a wider atmospheric control. Peings & Magnusdottir
475 (2014) suggest that atmospheric blocking prohibits the expected effects of the NAO on UK

476 and European hydrology, which may indirectly explain both the 1975-6 drought and the
477 disruption to the 7 year periodicity in UK groundwater (Rodda & Marsh 2011).

478 While the 16-32 year periodicity in groundwater level does, in general, align with historical
479 recorded droughts, this is not as coherent as with the 7 year cycle, with droughts occurring in
480 positive and negative phases. However, given the percentage contributions of the 16-32 year
481 periodicity to total groundwater variability, it is likely that this signal has a role in modulating
482 the severity of droughts influenced by the NAO 7-year drought cycle (as suggested by Comas-
483 Brua and McDermotta (2014)). For instance, the severe 1975-6 drought occurred at a slight
484 negative phase of the 16-32 year cycle, indicating that a portion of the severity of this drought
485 was the result of EA's influence.

486

487 Based on the alignment of the 7 year cycle (and partial alignment of the 16-32 year cycle) with
488 historical recorded UK droughts, we conclude that the NAO (and EA) directly modulate the
489 severity and timing of droughts in the UK. Furthermore, the 7-year cycle is shown to be a
490 sufficient indicator of the onset of droughts, based on this historical alignment. Consequently,
491 this 7-year cycle can be extrapolated beyond the end of the dataset used in this study.
492 Therefore, based on a projected 7-year cycle, we predict the UK will likely enter drought
493 conditions around 2018/19, 2025/6 and 2033/4, assuming the continuation of the NAO
494 system's influence. This projection is further validated by the onset of drought conditions in
495 the UK in mid-2018 (Hannaford, 2018).

496

497 In the UK, the economic regulator has implemented several measures to promote the trading
498 of water between water supply companies to enable a more robust water supply system
499 (OfWAT 2019; Deloitte LLP 2015). Here, we show that recursive patterns in groundwater
500 contribute to a considerable proportion of the total groundwater level variability and therefore
501 may provide new insights to allow undertakers of water supply to trade water further into the

502 future, depending on teleconnection sensitivities. Such forecasted planning could help to
503 reduce the ecological and human impacts of groundwater drought by allowing more time to
504 plan and organised the required water transfers from areas less susceptible to teleconnection-
505 driven drought.

506

507 **5. Conclusions**

508 This paper assesses the role of inter-annual variability and ocean-atmosphere systems in
509 influencing groundwater drought. We quantify, for the first time globally, the absolute
510 contribution of inter-annual cycles to groundwater variability, and provide new evidence for the
511 influence of the NAO's control of European rainfall on UK groundwater drought over the past
512 60 years.

513 The wavelet transformation was used to identify and evaluate bands of periodic external
514 influence on UK groundwater level hydrographs, documenting the strength of a 1, approximate
515 7 and 16-32 year cycle in the majority of sites assessed. We find that seasonality accounts for
516 an average of 39% of groundwater level variance across boreholes; with 7-year cycle
517 accounting for an average of 21%, and 16-32 years accounting for 15%. Furthermore, the
518 minima of NAO-driven cycles in groundwater level align with the occurrence of recorded
519 groundwater drought, allowing the estimation of future drought occurrences on a multi-annual
520 timescale. The analysis demonstrates that the NAO is the principle control (and the EA as the
521 secondary control) on inter-annual variability in UK groundwater level, and provides a new
522 approach to forecast the onset of groundwater droughts through an extrapolation of cyclical
523 behaviour into the future. As such we identify 2018/19, 2025/6 and 2033/4 as likely episodes
524 of future droughts in the UK. Although further work is required to better understand the
525 teleconnection sensitivity, the methods described in this paper provide a robust and
526 transferable approach for assessing the quantitative influence of teleconnections in
527 hydrological datasets. It is clear from our results that long-range groundwater drought

528 forecasts via climate teleconnections present transformational opportunities to drought
529 prediction and its management across the North Atlantic region.

530

531 **Acknowledgements**

532 This work was supported by the Natural Environment Research Council [grant number
533 NE/M009009/1], and the British Geological Survey (Natural Environment Research Council).
534 We acknowledge the British Geological Survey for provision of the groundwater level data,
535 and the Centre for Ecology and Hydrology for provision of the CHESS rainfall data
536 (https://doi.org/10.5285/33604ea0-c238-4488-813d-0ad9ab7c51ca) and CHESS PET data
537 (https://doi.org/10.5285/8baf805d-39ce-4dac-b224-c926ada353b7). John Bloomfield
538 publishes with the permission of the Executive Director, British Geological Survey (NERC).
539 Mark Cuthbert acknowledges support for an Independent Research Fellowship from the UK
540 Natural Environment Research Council (NE/P017819/1). We thank Angi Rosch and Harald
541 Schmidbauer for making their wavelet package “WaveletComp” freely available.

542 The groundwater level data used in the study are from the WellMaster Database in the
543 National Groundwater Level Archive of the British Geological Survey. The data are available
544 under license from the British Geological Survey at https:
545 //www.bgs.ac.uk/products/hydrogeology/WellMaster.html (last access: 26/03/2019).

546

547 **References**

548 Alexander, L. V., Tett, S.F.B. & Jonsson, T.: Recent observed changes in severe storms
549 over the United Kingdom and Iceland. Geophysical Research Letters, 32, 1–4,
550 https://doi.org/10.1029/2005GL022371, 2005.

551 Allen, M.R., Smith, L.A.: Monte Carlo SSA: Detecting irregular oscillations in the
552 Presence of Colored Noise. Journal of Climate, 9, 3373–3404, https://doi.org/10.1175/1520-
553 0442(1996)009<3373:MCSDIO>2.0.CO;2, 1996.

554 Bloomfield, J.P. & Marchant, B.P.: Analysis of groundwater drought building on the
555 standardised precipitation index approach. Hydrology and Earth System Sciences, 17, 4769–
556 4787, https://doi.org/10.5194/hess-17-4769-2013, 2013

557 Cuthbert, M.O., Gleeson, T., Moosdorf, N., Befus, K.M., Schneider, A., Hartmann, J. &
558 Lehner, B.: Global patterns and dynamics of climate–groundwater interactions. Nature Climate
559 Change, 9, 137–141, https://doi.org/10.1038/s41558-018-0386-4, 2019

560 Deloitte LLP: Water trading - scope, benefits and options - Final Report. Deloitte LLP,
561 117 pp, 2015.

562 Dickinson, J.E., Ferré, T.P.A., Bakker, M. & Crompton, B.: A Screening Tool for
563 Delineating Subregions of Steady Recharge within Groundwater Models. Vadose Zone
564 Journal, 13, 1-15, https://doi.org/10.2136/vzj2013.10.0184, 2014.

565 Faust, J.C., Fabian, K., Milzer, G., Giraudeau, J. & Knies, J.: Norwegian fjord
566 sediments reveal NAO related winter temperature and precipitation changes of the past 2800
567 years. Earth and Planetary Science Letters, 435, 84–93,
568 https://doi.org/10.1016/j.epsl.2015.12.003, 2016.

569 Ferguson, I.M. & Maxwell, R.M.: Role of groundwater in watershed response and land
570 surface feedbacks under climate change. Water Resources Research, 46(8), 1–15,
571 https://doi.org/10.1029/2009WR008616, 2010.

572 Folland, C.K., Hannaford, J., Bloomfield, J.P., Kendon, M., Svensson, C., Marchant,
573 B.P., Prior, J. & Wallace, E.: Multi-annual droughts in the English Lowlands: a review of their
574 characteristics and climate drivers in the winter half-year. Hydrology and Earth System
575 Sciences, 19, 2353–2375, https://doi.org/10.5194/hess-19-2353-2015, 2015.

576 Forootan, E., Khaki, M., Schumacher, M., Wulfmeyer, V., Mehrnegar, N., van Dijk,
577 A.I.J.M., Brocca, L., Farzaneh, S., Akinluyi, F., Ramillien, G., Shum, C.K., Awange, J. &
578 Mostafaie, A.: Understanding the global hydrological droughts of 2003–2016 and their
579 relationships with teleconnections. Science of the Total Environment, 650, 2587-260,
580 https://doi.org/10.1016/j.scitotenv.2018.09.231, 2018.

581 Fritier, N., Massei, N., Laignel, B., Durand, A., Dieppois, B. & Deloffre, J.: Links
582 between NAO fluctuations and inter-annual variability of winter-months precipitation in the
583 Seine River watershed (north-western France). Comptes Rendus - Geoscience, 344, 396–
584 405, https://doi.org/10.1016/j.crte.2012.07.004, 2012.

585 UK Hydrological Status Update - early July 2018: https://www.ceh.ac.uk/news-and-
586 media/blogs/uk-hydrological-status-update-early-july-2018, 2018.

587 Hauser, T., Demirov, E., Zhu, J. & Yashayaev, I.: North Atlantic atmospheric and
588 ocean inter-annual variability over the past fifty years - Dominant patterns and decadal shifts.
589 Progress in Oceanography, 132, 197–219,
590 https://doi.org/DOI: 10.1016/j.pocean.2014.10.008, 2015.

591 Holman, I., Rivas-Casado, M., Bloomfield, J.P. & Gurdak, J.J.: Identifying non-
592 stationary groundwater level response to North Atlantic ocean-atmosphere teleconnection
593 patterns using wavelet coherence. Hydrogeology Journal, 19, 1269–1278,
594 https://doi.org/10.1007/s10040-011-0755-9, 2011.

595 Holman, I.P., Rivas-Casado, M., Howden, N.J.K., Bloomfield, J.P. & Williams, A.T.:
596 Linking North Atlantic ocean-atmosphere teleconnection patterns and hydrogeological
597 responses in temperate groundwater systems. Hydrological Processes, 23, 3123–3126,
598 https://doi.org/10.1002/hyp.7466, 2009.

599 Hund, S. V., Allen, D.M., Morillas, L. & Johnson, M.S.: Groundwater recharge indicator
600 as tool for decision makers to increase socio-hydrological resilience to seasonal drought.
601 Journal of Hydrology, 563, 1119–1134, https://doi.org/10.1016/j.jhydrol.2018.05.069, 2018.

602 Hurrell, J.W. & Deser, C.: North Atlantic climate variability: The role of the North Atlantic
603 Oscillation. Journal of Marine Systems, 79, 231–244,
604 https://doi.org/10.1016/j.jmarsys.2008.11.026, 2010.

605 Hurrell, J.W., Kushnir, Y., Ottersen, G. & Visbeck, M.: An Overview of the North Atlantic
606 Oscillation. In The North Atlantic Oscillation: Climatic Significance and Environmental Impact.
607 American Geophysical Union, 1–35, 2003.

608 Jasechko, S., Birks, S.J., Gleeson, T., Wada, Y., Fawcett, P.J., Sharp, Z.D.,
609 McDonnell, J.J. & Welker, J.M.: The pronounced seasonality of global groundwater recharge.
610 Water Resources Research, 50, 8845–8867, https://doi.org/10.1002/2014WR015809, 2014.

611 Jelena Luković, Branislav Bajat, Dragan Blagojević, M.K.: Spatial pattern of North
612 Atlantic Oscillation impact on rainfall in Serbia. Spatial Statistics. 14, 39-52,
613 https://doi.org/10.1016/j.spasta.2015.04.007, 2014.

614 Kingston, D.G., McGregor, G.R., Hannah, D.M. & Lawler, D.M.: River flow
615 teleconnections across the northern North Atlantic region. Geophysical Research Letters, 33,
616 1–5, https://doi.org/10.1029/2006GL026574, 2006.

617 Knippertz, P., Ulbrich, U., Marques, F. & Corte-Real, J.: Decadal changes in the link
618 between El Niño and springtime North Atlantic oscillation and European–North African rainfall.
619 International Journal of Climatology, 23, 1293–1311, https://doi.org/10.1002/joc.944, 2003.

620 Krichak, S.O. & Alpert, P.: Decadal Trends in the East Atlantic-West Russia Pattern
621 and Mediterranean Precipitation. International Journal of Climatology. International Journal of
622 Climatology, 25, 183–192, https://doi.org/10.1002/joc.1124, 2005.

623 Kuss, A.M. & Gurdak, J.J.: Groundwater level response in U.S. principal aquifers to
624 ENSO, NAO, PDO, and AMO. Journal of Hydrology, 519, 1939–1952,
625 https://doi.org/10.1016/j.jhydrol.2014.09.069, 2014.

626 Lee, H.F. & Zhang, D.D.: Relationship between NAO and drought disasters in
627 northwestern China in the last millennium. Journal of Arid Environments, 75, 1114–1120,
628 https://doi.org/10.1016/j.jaridenv.2011.06.008, 2011.

629 López-Moreno, J.I., Vicente-Serrano, S.M., Morán-Tejeda, E., Lorenzo-Lacruz, J.,
630 Kenawy, A. & Beniston, M.: Effects of the North Atlantic Oscillation (NAO) on combined
631 temperature and precipitation winter modes in the Mediterranean mountains: Observed
632 relationships and projections for the 21st century. Global and Planetary Change, 77, 62–76,
633 https://doi.org/10.1016/j.gloplacha.2011.03.003, 2011.

634 Mackay, J.D., Jackson, C.R., Brookshaw, A., Scaife, A.A., Cook, J. & Ward, R.S.:
635 Seasonal forecasting of groundwater levels in principal aquifers of the United Kingdom.
636 Journal of Hydrology, 530, 815–828, https://doi.org/10.1016/j.jhydrol.2015.10.01, 2015.

637 Marsh, T., Cole, G. & Wilby, R.: Major droughts in England, 1800 - 2006. Weather, 62,
638 https://doi.org/10.1002/wea.67, 2007.

639 Marsh, T. & Hannaford, J.: UK Hydrometric Register. Hydrological data UK series.
640 Centre for Ecology and Hydrology, 214 pp, 2008.

641 Meinke, H., deVoil, P., Hammer, G.L., Power, S., Allan, R., Stone, R.C., Folland, C. &
642 Potgieter, A.: Rainfall variability of decadal and longer time scales: Signal or noise? Journal of
643 Climate, 18, 89–90, https://doi.org/10.1175/JCLI-3263.1, 2005.

644 Neves, M.C., Jerez, S. & Trigo, R.M.: The response of piezometric levels in Portugal
645 to NAO, EA, and SCAND climate patterns. Journal of Hydrology, 568, 1105–1117,
646 https://doi.org/10.1016/j.jhydrol.2018.11.054, 2019.

Water Trading: https://www.ofwat.gov.uk/regulated-companies/markets/water-bidding-market/water-trading, 2019.

Pasquini, A.I., Lecomte, K.L., Piovano, E.L. & Depetris, P.J.: Recent rainfall and runoff variability in central Argentina. Quaternary International, 158, 127–139, https://doi.org/10.1016/j.quaint.2006.05.021, 2006.

Peings, Y. & Magnusdottir, G.: Forcing of the wintertime atmospheric circulation by the multidecadal fluctuations of the North Atlantic Ocean. Environmental Research Letters, 9, 34018, http://dx.doi.org/10.1088/1748-9326/9/3/034018, 2014.

Peters, E., Bier, G., van Lanen, H.A.J. & Torfs, P.J.J.F.: Propagation and spatial distribution of drought in a groundwater catchment. Journal of Hydrology, 321, 257–275, https://doi.org/10.1016/j.jhydrol.2005.08.004, 2006.

Price, M., Downing, R.A. & Edmunds, W.M.: The chalk as an aquifer. In The hydeogeology of the Chalk of North-West Europe, Clarendon Press, Oxford, 2005.

Rashid, M.M., Beecham, S. & Chowdhury, R.K.: Assessment of trends in point rainfall using Continuous Wavelet Transforms. Advances in Water Resources, 82, 1-15, https://doi.org/10.1016/j.advwatres.2015.04.006, 2015.

Rey, D., Pérez-Blanco, C.D., Escriva-Bou, A., Girard, C. & Veldkamp, T.I.E.: Role of economic instruments in water allocation reform: lessons from Europe. International Journal of Water Resources Development, 35, 1–34, https://doi.org/10.1080/07900627.2017.1422702, 2018.

Robinson, E.L., Blyth, E., Clark, D.B., Comyn-Platt, E., Finch, J. & Rudd, A.C.: Climate hydrology and ecology research support system potential evapotranspiration dataset for Great Britain (1961 - 2015) [CHESS-PE], Centre for Ecology and Hydrology, https://doi.org/10.5285/8baf805d-39ce-4dac-b224-c926ada353b7, 2016.

671 Robinson, E.L., Blyth, E.M., Clark, D.B., Finch, J. & Rudd, A.C.: Trends in atmospheric
672 evaporative demand in Great Britain using high-resolution meteorological data, Hydrology and
673 Earth System Sciences, (21), 1189-1224, https://doi.org/10.5194/hess-21-1189-2017, 2017

674 Rodda, J. & Marsh, T.: The 1975-76 Drought - a contemporary and retrospective
675 review. Centre for Ecology and Hydrology, 2011.

676 Rosch, A. & Schmidbauer, H.: *WaveletComp 1.1: a guided tour through the R package,*
677 *2018.*

678 Rust, W., Holman, I., Corstanje, R., Bloomfield, J. & Cuthbert, M.: A conceptual model
679 for climatic teleconnection signal control on groundwater variability in Europe. Earth-Science
680 Reviews, 177, 164–174, https://doi.org/10.1016/j.earscirev.2017.09.017, 2018.

681 Su, L., Miao, C., Borthwick, A.G.L. & Duan, Q.: Wavelet-based variability of Yellow
682 River discharge at 500-, 100-, and 50-year timescales. Gondwana Research, 49, 94–105,
683 https://doi.org/10.1016/j.gr.2017.05.013, 2017.

684 Szolgayova, E., Parajka, J., Blo¨schl, G. & Bucher, C.: Long term variability of the
685 Danube River flow and its relation to precipitation and air temperature. Journal of Hydrology,
686 519, 871–880, https://doi.org/10.1016/j.jhydrol.2014.07.047, 2014.

687 Tanguy, M., Dixon, H., Prosdocimi, I., Morris, D. & Keller, V.D.J.: Gridded estimates of
688 daily and monthly areal rainfall for the United Kingdom (1890 - 2015) [CEH-GEAR]. Centre for
689 Ecology and Hydrology, https://doi.org/10.5285/33604ea0-c238-4488-813d-0ad9ab7c51ca,
690 2016.

691 Todd, B., Macdonald, N., Chiverrell, R.C., Caminade, C. & Hooke, J.M.: Severity,
692 duration and frequency of drought in SE England from 1697 to 2011. Climatic Change, 121,
693 673–687, https://doi.org/10.1007/s10584-013-0970-6, 2013.

694 Tošić, I., Zorn, M., Ortar, J., Unkašević, M., Gavrilov, M.B. & Marković, S.B.: Annual
695 and seasonal variability of precipitation and temperatures in Slovenia from 1961 to 2011.
696 Atmospheric Research, 168, 220–233, https://doi.org/10.1016/j.atmosres.2015.09.014, 2016.

697 Townley, L.R.: The response of aquifers to periodic forcing. Advances in Water
698 Resources, 18, 125–146, https://doi.org/10.1016/0309-1708(95)00008-7, 1995.

699 Tremblay, L., Larocque, M., Anctil, F. & Rivard, C.: Teleconnections and interannual
700 variability in Canadian groundwater levels. Journal of Hydrology, 410, 178–188,
701 https://doi.org/10.1016/j.jhydrol.2011.09.013, 2011.

702 Trigo, R.M., Pozo-Vazquez, D., Osborn, T.J., Castro-Diez, Y., Gamiz-Fortis, S. &
703 Esteban-Parra, M.J.: North Atlantic oscillation influence on precipitation, river flow and water
704 resources in the Iberian Peninsula. International Journal of Climatology, 24, 925–944,
705 https://doi.org/10.1002/joc.1048, 2004.

706 Van Loon, A.F.: Hydrological drought explained. Wiley Interdisciplinary Reviews:
707 Water, 2, 359–392, https://doi.org/10.1002/wat2.1085, 2015.

708 Van Loon, A.F.*On the propagation of drought: How climate and catchment*
709 *characteristics influence hydrological drought development and recovery*. Ph.D thesis.
710 Wageningen University, 2013.

711 Van Loon, A.F., Tijdeman, E., Wanders, N., Van Lanen, H.A.J., Teuling, A.J. &
712 Uijlenhoet, R.: How climate seasonality modifies drought duration and deficit. Journal of
713 Geophysical Research-Atmospheres, 119, 4640–4656,
714 https://doi.org/10.1002/2013JD020383, 2014.

715 Velasco, E.M., Gurdak, J.J., Dickinson, J.E., Ferré, T.P.A. & Corona, C.R.: Interannual
716 to multidecadal climate forcings on groundwater resources of the U.S. West Coast. Journal of
717 Hydrology: Regional Studies, 159, 16, https://doi.org/10.1016/j.ejrh.2015.11.018, 2015.

718 Wallace, J.M. & Gutzler, D.S.: Teleconnections in the Geopotential Height Field during
719 the Northern Hemisphere Winter. Monthly Weather Review, 109, 784–812,
720 https://doi.org/10.1175/1520-0493(1981)109%3C0784:TITGHF%3E2.0.CO;2, 1981.

721 Wang, H., Chen, Y., Pan, Y. & Li, W.: Spatial and temporal variability of drought in the
722 arid region of China and its relationships to teleconnection indices. Journal of Hydrology, 523,
723 283–296, https://doi.org/10.1016/j.jhydrol.2015.01.055, 2015.

724 Weber, K. & Stewart, M.: A Critical Analysis of the Cumulative Rainfall Departure
725 Concept, Groundwater, 42, 935-938, https://doi.org/10.1111/j.1745-6584.2004.t01-11-.x,
726 2004.

727